Climate response to increasing levels of greenhouse gases and sulphate aerosols

J. F. B. Mitchell, T. C. Johns, J. M. Gregory & S. F. B. Tett

Hadley Centre for Climate Prediction and Research, Meteorological Office, Bracknell RG12 2SY, UK

CLIMATE models suggest that increases in greenhouse-gas concentrations in the atmosphere should have produced a larger global mean warming than has been observed in recent decades, unless the climate is less sensitive than is predicted by the present generation of coupled general circulation models[1,2]. After greenhouse gases, sulphate aerosols probably exert the next largest anthropogenic radiative forcing of the atmosphere[3], but their influence on global mean warming has not been assessed using such models. Here we use a coupled ocean–atmosphere general circulation model to simulate past and future climate since the beginning of the near-global instrumental surface-temperature record[4], and include the effects of the scattering of radiation by sulphate aerosols. The inclusion of sulphate aerosols significantly improves the agreement with observed global mean and large-scale patterns of temperature in recent decades, although the improvement in simulations of specific regions is equivocal. We predict a future global mean warming of 0.3 K per decade for greenhouse gases alone, or 0.2 K per decade with sulphate aerosol forcing included. By 2050, all land areas have warmed in our simulations, despite strong negative radiative forcing in some regions. These model results suggest that global warming could accelerate as greenhouse-gas forcing begins to dominate over sulphate aerosol forcing.

The general circulation model (GCM) used is the Hadley Centre climate model, a development from an earlier model[5]. Modified formulations of the atmospheric dynamics[6], convection[7], land surface, boundary layer[8] and cloud[9] schemes have been used. The horizontal resolution is 2.5° × 3.75° (latitude × longitude), with 20 layers in the ocean and 19 layers in the atmosphere. We apply calibrated seasonal flux adjustments to ocean surface temperatures and salinities[5], to bring about a faithful representation of present mean climate. A simple parametrization of ice-drift[10] is included, obviating the need for flux adjustments to sea ice. The equilibrium sensitivity to a doubling of CO_2 concentration is estimated to be 2.5 K, lower than most GCMs[2].

The model was brought to near equilibrium through a total of 470 years coupled simulation, after which the control simulation commenced. There is no detectable trend in global mean surface temperature in the 300 model years of the control run, although there is a slow warming of the deeper ocean layers amounting to a maximum of 0.07 K per century in the global mean at 1,500 m depth. The net heating of the total system is less than 0.2 W m^{-2}.

Three experiments were performed, each starting at model year 1860: a control with constant CO_2 concentrations, an experiment GHG in which the concentration of CO_2 was increased gradually to give the changes in forcing due to all greenhouse gases, both in the past and to 2050 under a given scenario, and an experiment SUL in which both greenhouse gases and the direct radiative effect of sulphate aerosols were represented. The concentrations of sulphate aerosols and greenhouse gases after 1990 were based on IPCC scenario IS92a[2] which assumes a slow reduction in the rate of economic growth and gradual increase in conservation measures (Fig. 1).

The greenhouse-gas forcing increases slowly from 0.4 W m^{-2} relative to the control in 1860 to 1.2 W m^{-2} in 1960, then more rapidly reaching 2.5 W m^{-2} in 1990, and thereafter at 0.6 W m^{-2} per decade (Fig. 1*a*). The global mean sulphate aerosol forcing increases continuously, and most rapidly, from 1950 to 1990 (Fig. 1*a*). Note that in recent decades, the percentage increase per year of emissions has grown faster than the global average

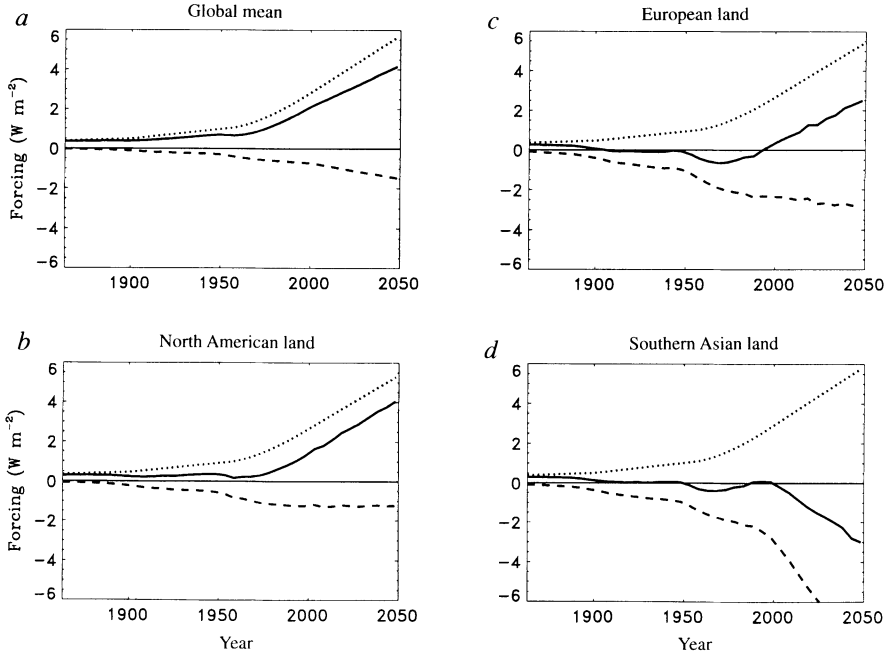

FIG. 1 Area-average annual mean radiative forcing owing to: increasing concentrations of greenhouse gases (experiment GHG, dotted curve); the direct effect of sulphate aerosols represented by increasing surface albedo (dashed curve); net forcing (experiment SUL, solid curve). *a*, The global mean; *b*, North America—land between 30° and 60° N and 40° to 140° W; *c*, Europe—land between 35° and 70° N and 15° W to 60° E; *d*, southern Asia—land between 7.5° and 42.5° N and 60° to 130° E.

METHODS. The concentration $C(t)$ of CO_2 at time t was chosen to give the estimated forcing (F) relative to the control (fixed concentration C_0) $F = 6.3 \ln(C(t)/C_0)$ W m^{-2} due to increases in all greenhouse gases from 1765 (ref. 2, Table 2.6). After 1990, $C(t)$ was increased by 1% yr^{-1}, which is within 0.2 W m^{-2} of IPCC scenario IS92a[2]. There is an initial increment of 0.4 W m^{-2} at 1860 arising from changes in greenhouse gas concentration from 1765 to 1860. The direct effect of sulphate aerosols was added in experiment SUL by increasing the surface albedo in the clear-sky fraction of each grid box[8,22]. The pattern of aerosol loading to 1990 was based on the calculated annual mean distribution for the 1980s[23], scaled by the estimated annual mean sulphate emissions[24,25]. The global mean forcing of 0.6 W m^{-2} at 1990 lies within recent estimates of 0.3–0.9 W m^{-2} (refs 18, 19). We have ignored seasonal variations of the pattern and the indirect effect of sulphate aerosols on cloud brightness[9]. A sulphate distribution for 2050 (H. Rodhe and U. Hansson, personal communication) was obtained using a sulphur-cycle model[23] with the sulphur emissions of scenario IS92a. From 1990 to 2050, the loading pattern was interpolated between 1990 and 2050 values, with the field scaled to give the global loading of scenario IS92a.

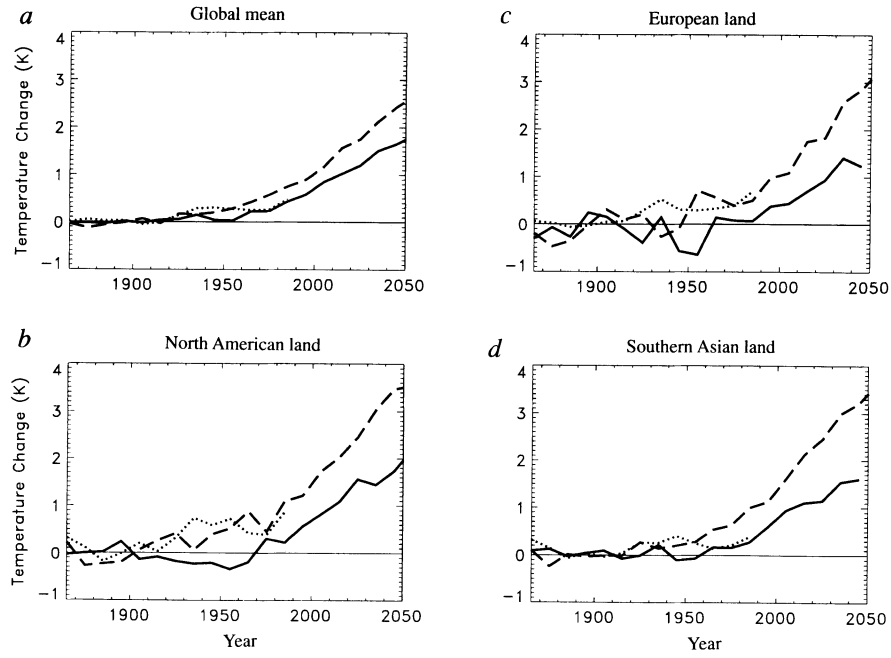

FIG. 2 Changes in area-average decadal mean temperature at 1.5 m, relative to the 1880–1920 mean. Observed[4] (dotted curve), GHG (dashed curve), SUL (solid curve). *a*, Global mean; *b*, mean over North America; *c*, mean over Europe; *d*, mean over southern Asia. Areas defined as in Fig. 1.

over southern Asia, and slower over western countries[11] where in the last decade there has been a decrease.

Reproduction of the past observational record within the limits of natural variability is a necessary, though not sufficient, condition for a model to produce reliable estimates of climate change. The differences in global mean temperature between simulations and observations[4] are within the range of simulated internal variability until about 1940 (Fig. 2*a*). The model's variability is generally greater than observed on timescales up to several decades. (On longer timescales, the estimates of internal variability based on the observations will be exaggerated by any long-term trend due to external forcing.) In the 1940s and 1950s, SUL is significantly cooler than the observations at the 5% significance level (two-tailed test assuming that decadal means are normally distributed with the same standard deviation, 0.073 K, as the control simulation). There is a 14% probability that at least two of the decades from 1860 to 1990 would be significantly different at this level by chance. Alternatively, the prescribed forcing (Fig. 1*a*) may be incorrect. The response to the 1.6 W m^{-2} change in forcing by 1990 in SUL is only 0.4 K, suggesting that it would require an increase in forcing of the order of 1 W m^{-2} to produce the extra warming in the 1940s. This seems unlikely, even with the large uncertainties in forcing[3]. For example, the optical depth of volcanic aerosols may have been a minimum[12], but the forcing anomaly was probably less than 0.5 W m^{-2}. A combination of natural fluctuations[13] and small errors in forcing seems the most likely explanation.

From 1970, the difference between GHG and observations[4] is significant in each decade at both the 5% (and 1%) levels whereas SUL is not significantly different from the observations at the 5% level after the 1930s and 1940s. Thus including the cooling attributed to sulphate aerosols (SUL) gives a simulation closer to the observations in recent decades, as found in energy-balance models[14–16] or idealized GCMs[17]. Note the rapid warming after 1970 in the observations and in SUL. In SUL, this is the response to accelerated greenhouse warming and a slower rate of increase in cooling from sulphate aerosols (Fig. 1*a*).

Comparison of the simulated spatial distribution of changes provides a potentially more stringent test of the model's credibility. We show decadal results starting with the 1860s, but focus mainly on the changes in recent decades when the observed data coverage is better and the forcing and signal-to-noise in the GHG and SUL experiments is largest (Figs 1, 2). We first compute decadal anomalies for GHG, SUL and the observations in the same manner by subtracting the respective 1860–1990 means from each decadal mean. Then we compute a centred spatial correlation for each successive decade between the model experiments and the observations. For the decades since 1950, the magnitude of the pattern correlation between SUL and the observations increases steadily, rising above the 10% significance

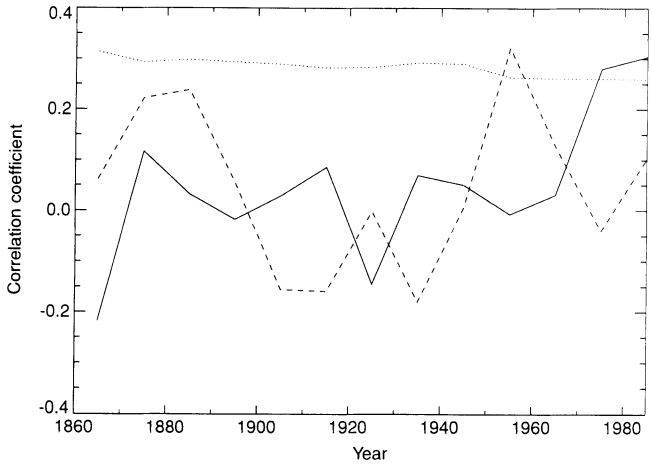

FIG. 3 Spatial correlation between simulated and observed decadal temperature changes relative to the 1860–1990 mean. Dashed line, GHG; solid line, SUL. The dotted line gives the 10% (one-tailed) level of significance, which varies with data coverage.

METHODS. Observed annual means were computed where there is at least one value in every month in a 5° grid-box. Observed and simulated data were averaged on a 15° × 15° grid, and decadal means formed in grid-boxes containing at least one annual observed value. The significance level was estimated from the distribution of correlations between decadal means in the control, assumed to be gaussian, using the observational mask for each decade.

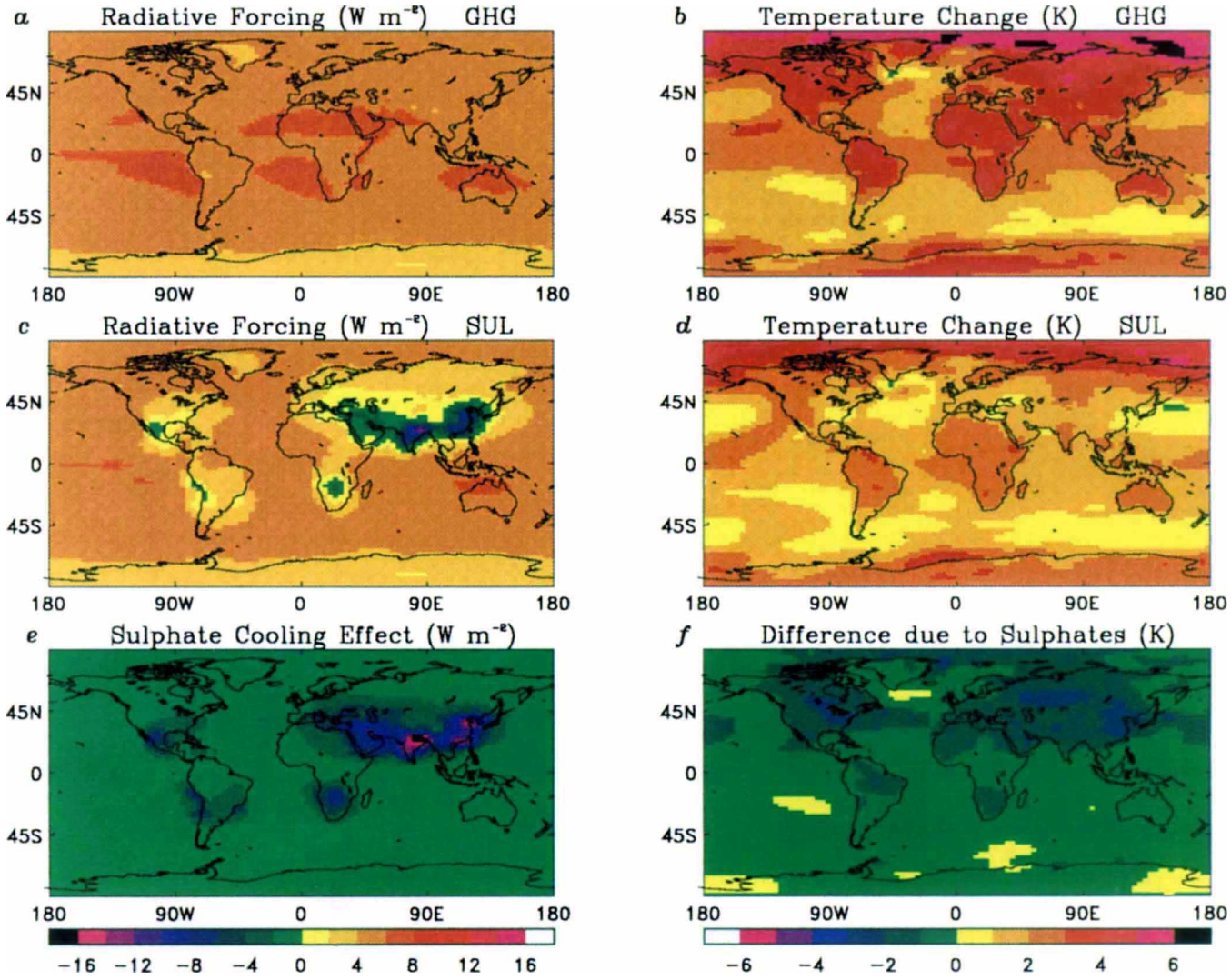

FIG. 4 Annual mean changes, averaged over 2030–50 relative to the control simulation. Temperature contours (*b*, *d*, *f* and right-hand scale bar) every 1 K, forcing contours (*a*, *c*, *e* and left-hand scale bar) every 2 W m^{-2}. *a*, *b*, Forcing (*a*) and temperature change (*b*) in GHG. *c*, *d*, Forcing (*c*) and temperature change (*d*) in SUL. *e*, *f*, Radiative cooling (*e*) and difference in response (*f*) due to adding sulphate aerosols. The greenhouse-gas forcing at year *t* is obtained by scaling the change at the top of the troposphere on instantaneously doubling CO_2 by ln ($C(t)$/C_0)/ln 2. The sulphate aerosol forcing is evaluated at the top of the atmosphere timestep by timestep.

level in the two most recent decades (Fig. 3). This recent trend is consistent with what could also be an emerging greenhouse gas/sulphate aerosol signal in the observations. The GHG correlation in the decade beginning in 1950 rises above the 10% significance level, but subsequent values are much smaller despite increasing forcing in the more recent decades. Thus the spatial patterns of surface temperature anomalies in SUL, compared to GHG, more closely resemble those in the observations in recent decades when the forcing is largest.

The distinction between the simulations is less evident in specific regions because of the high level of variability of temperature on smaller scales. GHG is substantially warmer than observed over southern Asia after 1960 (Fig. 2*d*). However, SUL is generally cooler than observed over Europe and North America after the 1940s (Fig. 2*b*–*d*). Possible explanations include excessive sulphate aerosol forcing in these regions and natural variability.

After 1990, the rate of global warming in GHG increases to 0.3 K per decade (Fig. 2*a*). In SUL, the rate increases rapidly to 0.2 K per decade, as the net forcing increases (Fig. 1*a*). Southern Asia continues to warm despite increasingly negative forcing (Fig. 1*d*), although at less than half the rate in GHG (Fig. 2*d*). Over North America and Europe, the aerosol forcing levels off and the greenhouse warming is more evident, though still less than in GHG. The increase in mean sulphate aerosol forcing still has a global effect, even where the local loading is substantially unchanged. The extension of these sensitivity studies to 2050 under a prescribed scenario indicates the potential strong influence of sulphate aerosols on regional climate change.

The patterns of forcing and response, averaged over 20 years from 2030, are shown in Fig. 4. The radiative forcing in GHG shows relatively little regional variation[18] (Fig. 4*a*). The response is enhanced in high latitudes by sea-ice feedbacks, and slowed in the Southern Ocean and the northern North Atlantic by deep mixing in the ocean (Fig. 4*b*), as in other transient experiments[2]. In SUL, there are areas of both positive and negative forcing (Fig. 1), but by 2030–50, areas of substantial net negative forcing are restricted to southern Asia (Fig. 4*c*). Even so, this region remains warmer than in the control simulation, due to the movement of warmer air from surrounding areas (Fig. 4*d*). The largest decreases in temperature on adding aerosols occur in northern mid-latitudes, where the forcing is largest, and in the Arctic, where the global-scale cooling is amplified by increases

in sea ice[8,19,20] (Fig. 4*e*, *f*). There is considerable variability on decadal and longer timescales—the standard deviation of 20-year means from the control simulation is 0.2–0.4 K over the extratropical continents—but the differences between GHG and SUL are several times larger than this and thus statistically significant. A more rigorous statistical assessment of the geographical distribution of changes will form a separate study.

We have shown that inclusion of sulphate aerosol forcing improves the simulation of global mean temperature over the last few decades, although further work is needed to clarify why the simulation over North America and Europe is not improved. There remain uncertainties in model sensitivity, particularly associated with clouds[21], and in the external forcing due to sulphate and other aerosols, tropospheric ozone and solar variability[3], and natural variability on long (greater than decadal) timescales. In particular, this study suggests that if we are to improve model predictions of climate change on global and regional scales it is not sufficient to consider greenhouse gases alone; the effects of aerosols and perhaps other forcing factors must be included. □

Received 27 January; accepted 12 July 1995.

1. Houghton, J. T., Jenkins, G. J. & Ephraums, J. J. (eds) *Climate Change. The IPCC Scientific Assessment*. (Cambridge Univ. Press, 1990).
2. Houghton, J. T., Callander, B. A. & Varney, S. K. (eds) *Climate Change 1992. The Supplementary Report to the IPCC Scientific Assessment* (Cambridge Univ. Press, 1992).
3. Houghton, J. T. *et al.* (eds) *Climate Change 1994, Radiative Forcing of Climate Change, and an Evaluation of the IPCC IS92 Emission Scenarios* (Cambridge Univ. Press, 1995).
4. Parker, D. E., Jones, P. D., Folland, C. K. & Bevan, A. *J. geophys. Res.* **99,** 14373–14399 (1994).
5. Murphy, J. M. *J. Clim.* **8,** 36–56 (1995).
6. Cullen, M. J. P. & Davies, T. R. *Q. J. R. met. Soc.* **117,** 993–1002 (1991).
7. Gregory, D. & Allen, S. in *Preprints 9th Conf. on Numerical Weather Prediction* 122–123 (American Meteorological Soc., Boston, 1991).
8. Mitchell, J. F. B., Davis, R. A., Ingram, W. J. & Senior, C. A. *J. Clim.* (in the press).
9. Jones, A., Roberts, D. L. & Slingo, A. *Nature* **369,** 450–453 (1994).
10. Bryan, K. *Mon. Weath. Rev.* **97,** 806–827 (1969).
11. Engardt, M. & Rodhe, H. *Geophys. Res. Lett.* **20,** 117–120 (1993).
12. Sato, M., Hansen, J. E., McCormick, M. P. & Pollack, J. B. *J. geophys. Res.* **98,** 22987–22994 (1993).
13. Schlesinger, M. E. & Ramankutty, N. *Nature* **367,** 723–726 (1994).
14. Wigley, T. M. L. & Raper, S. C. B. *Nature* **357,** 293–300 (1992).
15. Schlesinger, M. E., Jiang, X. & Charlson, R. J. in *Climate Change and Energy Policy* (eds Rosen, L. & Glasser, R.) 75–108 (Am. Inst. Phys., New York, 1993).
16. Murphy, J. M. *J. Clim.* **8,** 496–514 (1995).
17. Hansen, J., Lacis, A., Reudy, R. & Wilson, H. *Nat. Geogr. Explor.* **9,** 142–158 (1993).
18. Kiehl, J. T. & Briegleb, P. B. *Nature* **260,** 311–314 (1993).
19. Taylor, K. & Penner, J. E. *Nature* **369,** 734–737 (1994).
20. Roeckner, E., Siebert, T. & Feichter, J. in *Proc. Dahlem Workshop* on *Aerosol Forcing of Climate* (eds Charlson, R. J. & Heintsenberg, J.) (Wiley, in the press).
21. Senior, C. A. & Mitchell, J. F. B. *J. Clim.* **6,** 393–418 (1993).
22. Charlson, R. J., Langner, J., Rodhe, H., Leovy, C. B. & Warren, S. G. *Tellus* **43AB,** 152–163 (1991).
23. Langner, J. & Rodhe, H. *J. atmos. Chem.* **13,** 225–263 (1991).
24. Dignon, J. & Hameed, S. *J. Air Pollut. Control Ass.* **39,** 180–186 (1989).
25. Hameed, S. & Dignon, J. *J. Air Pollut. Control Ass.* **42,** 159–186 (1992).

ACKNOWLEDGEMENTS. We thank H. Rodhe and U. Hansson for providing the estimates of sulphate distribution, D. E. Parker for observational data, and G. Meehl and our colleagues for helpful comments. R. Davis, A. Brady and J. Lavery assisted with running the experiments and processing data. This work was supported by the UK Department of Environment.

Glacial climate instability in the Northeast Pacific Ocean

Robert C. Thunell* & P. Graham Mortyn*†

* Department of Geological Sciences, University of South Carolina, Columbia, South Carolina 29208, USA

RECENT climate records from Greenland ice cores[1,2] and North Atlantic sediments[3–5] have challenged the long-held notion that Pleistocene climate fluctuates between two relatively stable states (glacials and interglacials). It has been appreciated for some time that the transitions from one state to another are not smooth[6], but the new records indicate that the glacial and interglacial periods themselves appear to be punctuated by significant climate variability—several short interstadial events punctuated the last glacial period, for example. But it has not been clear whether this climate instability is a global phenomenon or is peculiar to the North Atlantic region. Here we present climate proxy records from sediment cores from the eastern margin of the North Pacific Ocean, which indicate that climate in this region was also highly unstable during the last glaciation. Our observations suggest that glacial climate instability throughout the Northern Hemisphere might be linked to rapid changes in the size of the Laurentide ice sheet and associated changes in atmospheric circulation.

There is no clear consensus as to the origin of the observed climate instability that marks the last glacial period. Are the rapid shifts from one climate state to another the result of internal or external forcing? Broecker *et al.*[7,8] were the first to suggest that the rapid climate changes observed in Greenland ice cores represent shifts between two climate modes and that these fluctuations were the result of turning on and off the North Atlantic thermohaline circulation. As an alternative to changes in the ocean–atmosphere system, a model has been proposed in which internal ice-sheet dynamics generated cyclical changes in the size of the Laurentide ice sheet and that these ice volume changes caused the observed instability in North Atlantic climate during the last glacial[9,10].

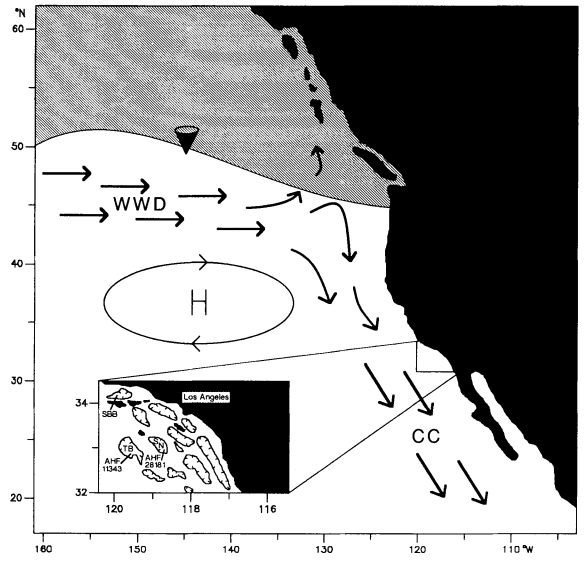

FIG. 1 Main figure, map of the northeast Pacific showing the location of the North Pacific high-pressure centre (H), and the major surface currents (CC, California Current; WWD, West Wind Drift). The lightly shaded area represents the present-day range of left-coiling *N. pachyderma* (based on Be[11]). The southern boundary of this range is approximately the winter position of the 8 °C surface-water isotherm. The location of our previous subpolar North Pacific sediment-trap study[12] is indicated by the cone. Inset, the locations of the two California Borderlands cores used in this study (TB, Tanner basin; SN, San Nicolas basin).

We have conducted a detailed micropalaeontological study of two cores from the Tanner and San Nicolas basins of the California Borderlands region (Fig. 1) in order to evaluate climate variability in the northeast Pacific during the last glacial period. In particular, we use changes in the abundance of the planktonic

† Present address: Scripps Institution of Oceanography, University of California, San Diego, La Jolla, California 92093, USA.